On Small Multi-Dimensional Constellations For Nonlinear Optical Fiber Communications

Junho Cho[(1)] and Xi Chen[(1)]

[(1)] Nokia Bell Labs, Holmdel, NJ, USA, {junho.cho, xi.v.chen}@nokia-bell-labs.com

Abstract *We review three small multi-dimensional constellations with an information rate of 1 bit/dimension or less in a concatenated coded modulation framework and compare the gain and loss of multi-dimensional coding through optical transmission simulations.*

Introduction

There have been various approaches to mitigate nonlinear impairments in wavelength-division multiplexed (WDM) optical fiber communications by using modulation techniques. For example, transmission of phase-conjugated twin waves (PCTW) on two polarizations[1] allowed to digitally cancel self-phase modulation (SPM) at the receiver through polarization diversity combining. Alamouti-coded modulation (ACM)[2] was demonstrated to suppress polarization scattering induced by cross-phase modulation (XPM) as well as SPM. Various multi-dimensional (MD) modulations[3] have also been used to withstand nonlinear phase noise (NLIN) due to SPM and XPM; for example, the 8D polarization-balanced (8D-PB) modulation[4] and the 4D 64-ary polarization-ring-switching (4D-64PRS) modulation[5] were demonstrated to reduce manifestation of the NLIN caused by polarization rotation[6] and the fourth-order moment of modulation symbols[6], respectively.

In this paper, we analyze various MD modulations proposed for optical fiber communications. By interpreting the MD modulation as a concatenated coded modulation scheme, we show that the MD modulation should be evaluated *not* only from the enhanced effective signal-to-noise ratio (SNR_{eff}) in optical fiber channels *but* also from the increased coding gap in auxiliary additive white Gaussian noise (AWGN) channels. For the sake of simplicity, we restrict the scope of the paper to small MD constellations whose projection onto each dimension is a binary phase-shift keying (BPSK) constellation (hence produces an information rate (IR) $\leq$ 1 b/D), although similar analysis can be applied to larger constellations. We show by simulation that the small MD modulations under investigation enhance SNR_{eff}, but the loss in coding gain outweighs the enhancement in SNR_{eff}, thereby leading to a smaller IR than 1D modulation.

MD Constellations with IR $\leq$ 1 b/D

Fig. 1(a) shows a typical coded modulation system for square quadrature amplitude modulation (QAM) constellations, which consists of forward error correction (FEC) coding and 1D bit-to-symbol mapping. On the other hand, the three MD modulations of our interest (i.e., PCTW, ACM, and 8D-PB) use a different architecture as shown in Fig. 1(b), which has an additional coding layer relative to Fig. 1(a).

The PCTW scheme[1] sends a complex-valued information symbol u on x-polarization and its conjugate u^* on y-polarization, hence builds a 4D constellation in each time slot in polarization-division multiplexed (PDM) transmission, where $u \in \{\pm 1 \pm j\}$ in this paper. Note that if bits $[b_1, b_2]$ are mapped by Φ to u, the bits that are mapped to the conjugate symbol u^* are $[b_1, \bar{b}_2]$, where $\bar{b}$ denotes negation of b. Therefore, MD mapping of the PCTW scheme is realized by a binary encoding function f that transforms $[b_1, b_2]$ into $[b_1, b_2, b_1, \bar{b}_2]$ (cf. Tab. 1), followed by mapping Φ. The encoding f is a (variant of) repetition coding that sends the same information bit two times, resulting in 3-dB increase in signal power per information bit (hence also in SNR_{eff} per bit). The encoding function f is not linear in its current form, but can be converted to a linear form using the relation $\bar{b} = 1 \oplus b$, where $\oplus$ denotes modulo-2 addition. Following the notational convention

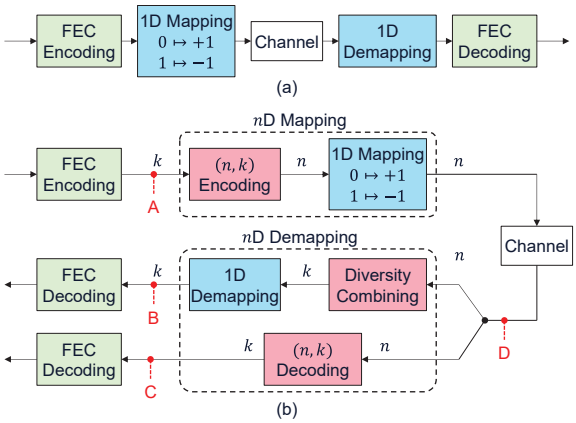

Fig. 1: Coded modulation system with (a) a 1D constellation, and (b) an nD constellation.

Tab. 1: Encoding functions for MD modulations

MD Modulation	Encoding Function	(n, k, d_H)
PCTW	$b_1 b_2 \rightarrow b_1 b_2 b_1 \bar{b}_2$	(4,2,2)
ACM	$b_1 b_2 b_3 b_4 \rightarrow b_1 b_2 b_3 b_4 \bar{b}_3 b_4 b_1 \bar{b}_2$	(8,4,3)
8D-PB	$b_1 b_2 b_3 b_4 \rightarrow b_1 b_2 b_3 b_4 p_1 p_2 \bar{p}_3 \bar{p}_4$ $p_1 = b_2 \oplus b_3 \oplus b_4$ $p_2 = b_1 \oplus b_3 \oplus b_4$ $p_3 = b_1 \oplus b_2 \oplus b_4$ $p_4 = b_2 \oplus b_2 \oplus b_3$	(8,4,4)

which represents a code of length n, information length k, and minimum Hamming distance d_H as an (n, k, d_H) code, the PCTW scheme implements a $(4,2,2)$ code by adding 2-bit *redundancy* per 2-bit information. At the receiver side, given demultiplexed symbols $[v_1, v_2]$ on x- and y-polarizations in order, u can be recovered through diversity combining as $\tilde{u} \approx (v_1 + v_2^*)/2$, as shown in the upper signal flow of Fig. 1(b). This diversity combining rule can partially cancel SPM-induced NLIN, hence the PCTW increases SNR_{eff} by $\geq$ 3 dB, compared to PDM quadrature phase-shift keying (QPSK). Instead, MD demapping can be performed in the form of soft-input soft-output maximum-likelihood (ML) decoding of an (n, k) code, as shown in the lower signal flow of Fig. 1(b); namely, we can obtain the log-likelihood ratio (LLR) of the i-th bit for $i = 1, \ldots, k$, as $L_i = \log\{\sum_{\boldsymbol{u}\in\boldsymbol{\mathcal{X}}_i^0} \exp[-\|\boldsymbol{v}-\boldsymbol{u}\|^2/(2\sigma^2)]\} / \sum_{\boldsymbol{u}\in\boldsymbol{\mathcal{X}}_i^1} \exp[-\|\boldsymbol{v}-\boldsymbol{u}\|^2/(2\sigma^2)]\}$, where $\boldsymbol{u}$ and $\boldsymbol{v}$ are the nD transmitted and received symbols, respectively, $\boldsymbol{\mathcal{X}}_i^0$ and $\boldsymbol{\mathcal{X}}_i^1$ are the sets of nD constellation points whose i-th bit level is 0 and 1, respectively, and σ^2 is the noise variance per dimension of the auxiliary AWGN channel.

The ACM scheme[2] transmits two complex information symbols $[u_1, u_2]$ in one time slot, and then transmits their altered copies $[-u_2^*, u_1^*]$ in the next time slot. The ACM therefore builds an 8D constellation that spans 2 PDM time slots. In the framework of Fig. 1(b), the ACM scheme consists of $(8,4,3)$ repetition coding $f: [b_1, b_2, b_3, b_4] \rightarrow [b_1, b_2, b_3, b_4, \bar{b}_3, b_4, b_1, \bar{b}_2]$ (cf. Tab. 1) followed by mapping Φ. If we denote the stokes parameters of a PDM symbol $[u_1, u_2]$ by $S_0 = |u_1|^2 + |u_2|^2$, $S_1 = |u_1|^2 - |u_2|^2$, $S_2 = 2Re[u_1 u_2^*]$, $S_3 = 2Im[u_1 u_2^*]$, and define the degree of polarization (DOP) for a block of symbols spanning N time slots as $DOP \coloneqq \sqrt{\langle S_1\rangle_N^2 + \langle S_2\rangle_N^2 + \langle S_3\rangle_N^2}/\langle S_0\rangle_N$, with $\langle\cdot\rangle_N$ being the average over N time slots, it can be shown that all ACM symbols produce zero DOP (0-DOP) in 8D (i.e., with $N = n/4 = 2$). This brings an effect of sending *block-wise unpolarized* PDM symbols in every 2 time slots, and mitigates polarization-rotation-induced NLIN, thereby enhancing SNR_{eff}. The encoding f also increases d_H by 2 bits in each 8D (cf. Tab. 1) compared to QPSK, at the expense of 1-b/D overhead. The diversity combining rule at the receiver is $\tilde{u}_1 \approx (v_1 + v_4^*)/2$ and $\tilde{u}_2 \approx (v_2 - v_3^*)/2$, where $[v_1, v_2]$ and $[v_3, v_4]$ denote the polarization-demultiplexed symbols on the 1st and 2nd time slots, respectively.

Like the ACM, the 8D-PB scheme[4] achieves 0-DOP in each 8D, but using a different encoding rule. The 8D-PB encoding of Ref. [4] is equivalent to $(8,4,4)$ extended Hamming encoding, where the last 2 bits of the codewords (p_3, p_4 in Tab. 1) are flipped to fulfill the 0-DOP condition. We can expect the same SNR_{eff} from the ACM and 8D-PB, since they both attain 0-DOP in 8D and a constant modulus in 4D. However, the 8D-PB encoding realizes 1-bit larger d_H than the ACM. In our setup, the minimum Euclidean distance d_E increases with d_H as $d_E = 2\sqrt{d_H}$ in nD. This leads to different IRs for the ACM and 8D-PB, as shown in the following section. At the receiver side, only allowed is the MD demapping for 8D-PB, as there is no diversity combining rule.

The decomposition of MD modulations into coding and 1D modulation may look similar to the approach of Ref. [3]; however, the coding in this paper is not restricted to be linear, and we evaluate the modulations in terms of the IR by taking into account the coding redundancy, instead of the sphere-packing performance. This evaluation is in line with the idea of Ref. [7] that considers reduced entropies of MD modulations on each 1D-projected constellation.

Numerical Evaluation

If one would evaluate the gain of MD modulations in terms of the pre-FEC bit error rate (BER), as is often done in optical systems characterization, care should be taken to measure the BER *not* at point B or C in Fig. 1(b) after MD demapping, *but* at point D (after 1D demapping, not shown in Fig. 1(b)). This is because the MD demapping involves decoding of a length-n inner code, implying that the BER at point B or C is indeed a *post-FEC BER*. Even at point D, however, the BER is not a proper metric to assess soft-decision demapping and decoding. Therefore, for general systems with either hard- or soft-decision decoding, SNR_{eff} should be measured at point D, which is a *sufficient statistic* for the auxiliary AWGN channel of the true optical fiber channel. On the other hand, the generalized mutual information (GMI)[8] that represents an achievable IR of our system should be measured at point B or C, with respect to the transmitted bits at point A.

To compare various modulations, we perform nonlinear fiber transmission simulations based on the split-step Fourier method, using TrueWave REACH fiber[9] with average loss of 0.20 dB/km, low dispersion of 7.44 ps/nm/km, and small effective area of 55 μm^2. The simulated link consists of 80-km spans. In order to aggravate the nonlinear impairment, chromatic dispersion is ideally compensated at the end of every span. Nine channels of 45-GBaud symbols with the same modulation format are transmitted through fiber at 50-GHz spacing, and the performance of the center channel at 1550 nm is evaluated. Root raised cosine (RRC) pulse shaping is applied at the transmitter with a roll-off factor of 0.1.

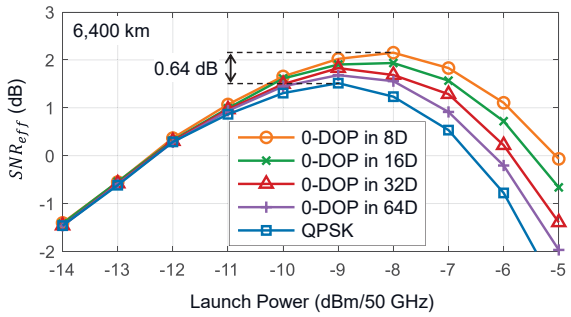

Fig. 2: Impact of the block length for 0-DOP on SNR_{eff}.

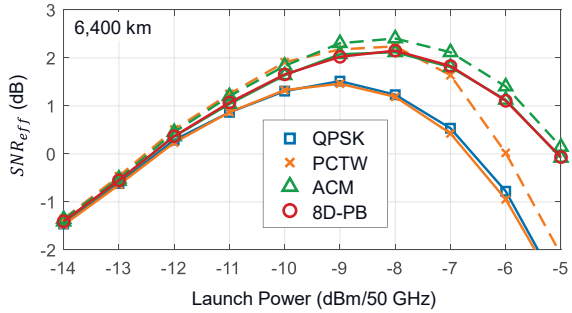

Fig. 3: SNR_{eff} of various modulations. Solid line: without diversity combining, dashed line: after diversity combining.

To see how much 0-DOP mitigates the polarization-rotation-induced NLIN, we transmit nD modulation symbols that realize 0-DOP in each nD, with $n = 8, 16, 32, 64$; i.e., the PDM symbols are block-wise unpolarized in every $N = n/4 = 2, 4, 8, 16$ time slots. Note that the smallest n that can attain 0-DOP is 8. Fig. 2(a) shows SNR_{eff} of 0-DOP modulations with various block sizes at 4,800 km. It can be seen that: *(i)* SNR_{eff} is enhanced as the 0-DOP block length decreases, and *(ii)* the SNR_{eff} gain from 0-DOP modulations reaches only up to 0.7 dB even in our substantially nonlinear link configuration.

Fig. 3 shows SNR_{eff} of the three MD modulations under test, as well as that for the QPSK, at 4,800 km. The solid lines show SNR_{eff} measured at point D of Fig. 2(b), and the dashed lines are SNR_{eff} obtained by diversity combining (where applicable) subtracted by 3 dB to exclude the two-times larger signal power per information symbol and see only the gain from NLIN mitigation. As seen from the figure, the PCTW produces similar SNR_{eff} at point D (crosses, solid line) to QPSK (squares), implying that it does not prevent manifestation of NLIN, but rather cancels some of the NLIN at the receiver by diversity combining (crosses, dashed line). The ACM (triangles, solid line) and 8D-PB (circles, solid line), on the other hand, which are nearly indistinguishable in Fig. 3 yield a greater SNR_{eff} than QPSK at point D, showing that they reduce the NLIN arising from the fiber.

Recall, however, that the SNR_{eff} curves in Figs. 2 and 3 are obtained with different amount

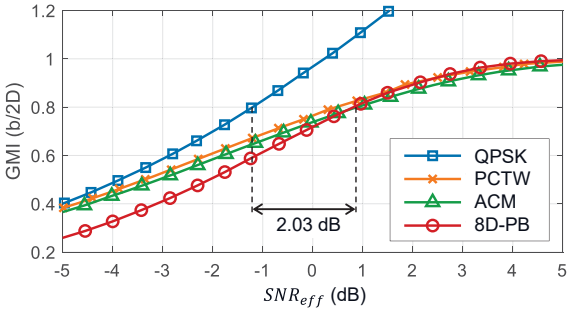

Fig. 4: GMI as a function of SNR_{eff}.

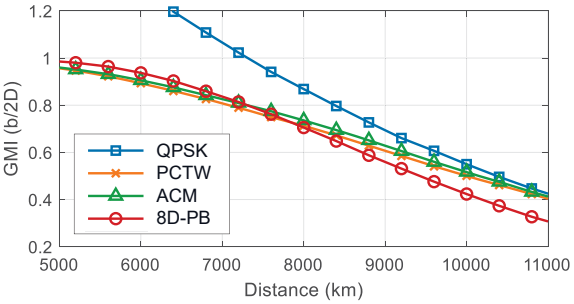

Fig. 5: GMI as a function of distance, with optimized launch powers at each distance.

of overhead. Shown in Fig. 4 is the GMI that takes all the overhead into account. The GMI measured with the symbols at points A and C of Fig. 1(b) (without diversity combining) is only shown, since diversity combining yields a difference of no larger than 0.005 b/D in GMI compared to (n, k) decoding. Interestingly, QPSK produces the greatest GMI at almost all distances. This indicates that the MD modulations use the inner coding overhead less efficiently than the FEC code of QPSK, and the coding gap increased by the inner coding outweighs the gain in SNR_{eff} resulting from the decrease in NLIN, even in our substantially nonlinear channel. The inefficiency of inner coding originates fundamentally from a short code length of 4 or 8, which is a constraint favored by optical fiber propagation physics. Note also that, although the 8D-PB produces similar SNR_{eff} to those of the ACM at all distances and has a larger d_H than the ACM, the 8D-PB produces a smaller GMI than the ACM at distances $>$ 5,200 km (at $SNR_{eff} <$ ~0.5 dB). This may seem surprising, but it is a natural consequence of the fact that a single MD symbol error creates more bit errors as d_H increases, if SNR_{eff} is below a certain value. This shows that the existing approaches to design MD modulations for a large d_H are not necessarily optimal.

Conclusion

We reviewed three small MD modulations in a concatenated coded modulation framework, and showed by optical transmission simulations in a dispersion-unmanaged link that the reduction in coding efficiency of the MD modulations outweighs the increase in effective SNR.

References

[1] X. Liu et al., “Phase-conjugated twin waves for communication beyond the Kerr nonlinearity limit,” *Nature Photon.,* vol. 7, no. 7, pp. 560–568, May 2013.

[2] Y. Han and G. Li, “Polarization diversity transmitter and optical nonlinearity mitigation using polarization-time coding,” in *Proc. Coherent Opt. Technol. Appl.*, Whistler, Canada, Jun., 2006, Paper CThC7.

[3] D. S. Millar et al., “High-dimensional modulation for coherent optical communications systems,” *Opt. Express*, vol. 22, no. 7, pp. 8798–8812, Apr. 2014.

[4] A. D. Shiner et al., “Demonstration of an 8-dimensional modulation format with reduced inter-channel nonlinearities in a polarization multiplexed coherent system,” *Opt. Express*, vol. 22, no. 17, pp. 20366–20374, Aug. 2014.

[5] B. Chen et al., “Polarization-ring-switching for nonlinearity-tolerant geometrically shaped four-dimensional formats maximizing generalized mutual information,” *J. Lightw. Technol.*, vol 37, no. 14, 3579–3591, Jul. 2019.

[6] R. Dar and P. J. Winzer, “Nonlinear interference mitigation: Methods and potential gain,” *J. Lightw. Technol.*, vol. 35, no. 4, pp. 903–930, Feb. 2017.

[7] J. C. Cartledge et al., “Digital signal processing for fiber nonlinearities,” Opt. Express, vol. 25, no. 3, pp. 1916–1936, Feb. 2017.

[8] A. Alvarado et al., “Replacing the soft FEC limit paradigm in the design of optical communication systems,” *J. Lightw. Technol.*, vol. 33, no. 20, pp. 4338–4352, Oct. 2015.

[9] OFS, “TrueWave REACH optical fiber,” 2017. [Online]. Available: https://www.ofsoptics.com/wp-content/uploads/TrueWaveREACHFiber-124-web-4.pdf.